

# Construction of a generalized gradient approximation by restoring the density-gradient expansion and enforcing a tight Lieb–Oxford bound

Yan Zhao<sup>a)</sup> and Donald G. Truhlar<sup>b)</sup>

*Department of Chemistry and Supercomputing Institute, University of Minnesota, 207 Pleasant Street, S.E. Minneapolis, Minnesota 55455-0431, USA*

(Received 26 February 2008; accepted 27 March 2008; published online 14 May 2008)

Recently, a generalized gradient approximation (GGA) to the density functional, called PBEsol, was optimized (one parameter) against the jellium-surface exchange-correlation energies, and this, in conjunction with changing another parameter to restore the first-principles gradient expansion for exchange, was sufficient to yield accurate lattice constants of solids. Here, we construct a new GGA that has no empirical parameters, that satisfies one more exact constraint than PBEsol, and that performs 20% better for the lattice constants of 18 previously studied solids, although it does not improve on PBEsol for molecular atomization energies (a property that neither functional was designed for). The new GGA is exact through second order, and it is called the second-order generalized gradient approximation (SOGGA). The SOGGA functional also differs from other GGAs in that it enforces a tighter Lieb–Oxford bound. SOGGA and other functionals are compared to a diverse set of lattice constants, bond distances, and energetic quantities for solids and molecules (this includes the first test of the M06-L meta-GGA for solid-state properties). We find that classifying density functionals in terms of the magnitude  $\mu$  of the second-order coefficient of the density gradient expansion of the exchange functional not only correlates their behavior for predicting lattice constants of solids versus their behavior for predicting small-molecule atomization energies, as pointed out by Perdew and co-workers [Phys. Rev. Lett. **100**, 134606 (2008); Phys. Rev. Lett. **80**, 891 (1998)], but also correlates their behavior for cohesive energies of solids, reaction barriers heights, and nonhydrogenic bond distances in small molecules. © 2008 American Institute of Physics. [DOI: 10.1063/1.2912068]

## I. INTRODUCTION

Since the birth of Kohn–Sham density functional theory (DFT),<sup>1</sup> the local spin density approximation (LSDA) and generalized gradient approximation (GGA) have been widely applied in solid-state physics,<sup>2</sup> with the most popular GGA being that of Perdew, Burke, and Ernzerhof<sup>3</sup> (PBE). Although hybrid functionals<sup>4–7</sup> (which include Hartree–Fock exchange) and meta-GGAs (Refs. 7–11) (which include spin kinetic energy density<sup>8,12</sup>) have also been developed and have been popularly and successfully applied in molecular quantum chemistry during the past decade, they are not widely used in solid-state physics, and very few solid-state codes have the capability of performing calculations with meta-GGAs or hybrid functionals. In the present work, we focus on the development of an accurate GGA for solids. We will, however, also include some molecular properties and meta-GGAs in our discussion in order to provide perspective.

Some modifications of the popular PBE functional such as RPBE (Ref. 13) and revPBE (Ref. 14) improve the atomization energies of molecules but worsen the results for lattice constants.<sup>15</sup> Some other modifications of PBE, such as the Wu–Cohen,<sup>16</sup> PBE $\alpha$ ,<sup>15</sup> and PBEsol<sup>17</sup> functionals, improve the results for solids but worsen the performance for atomi-

zation energies. The recent work of Perdew and co-workers<sup>17,18</sup> showed that it is impossible for a GGA to perform well for certain pairs of properties, e.g., both for molecular atomization energies and for lattice constants of solids.

Some of these results can be rationalized in terms of the gradient expansion of the exchange and correlation functional, but before considering this, it is worthwhile to remind ourselves that a GGA is, by definition, a functional of only the up and down spin densities and the magnitudes of their gradients. This is a very restrictive form (chosen more for convenience than for fundamental reasons), and it can be shown that a GGA cannot be exact, in general, for either exchange or correlation.<sup>19</sup> Furthermore, the second-order expansion of the GGA with best performance for one or more selected properties need not be the same as the (known) second-order expansion of the (unknown) true density functional even in its region of applicability. Consistently with this perspective, Perdew *et al.*<sup>17</sup> have shown that accurate atomic exchange energies (important for atomization energies of molecules) require violating the gradient expansion for slowly varying densities (important for solids). In the recent PBEsol model, Perdew *et al.*<sup>17</sup> restored the gradient expansion for exchange but violated the gradient expansion for correlation by fitting a parameter in the correlation functional for the jellium exchange-correlation (XC) surface en-

<sup>a)</sup>Electronic mail: zhaoy@comp.chem.umn.edu.

<sup>b)</sup>Electronic mail: truhlar@umn.edu.

ergy. In the GGA developed in the present work, we enforce a complete restoration of the gradient expansion for exchange and correlation.

One of the parameters in the PBE exchange functional<sup>3</sup> was determined by enforcing the Lieb–Oxford<sup>20</sup> bound. The Lieb–Oxford bound is an upper limit on the ratio  $\lambda$  of the exact exchange–correlation energy of a system to the value of the LSDA approximation to the exchange energy of the system (both of the values being ratioed are intrinsically negative). Recently, Odashima and Capelle<sup>21</sup> examined the value of  $\lambda$  for a number of atoms, ions, and molecules, one solid, and some model Hamiltonians. Their work suggests that the Lieb–Oxford bound could be substantially tightened. In the GGA developed in the present study, we enforce a tighter Lieb–Oxford bound. Csonka *et al.*<sup>22</sup> have, in fact, explored the effect of more tightly bounded exchange. The present study incorporates a tighter Lieb–Oxford bound on a GGA that in other respects restores theoretically preferred behavior that had been violated on the basis of the perceived requirements of competing practical concerns.

Another subject of the present work is to assess the performance of the M06-L<sup>10</sup> density functional for the prediction of lattice constants of solids. M06-L is a meta-GGA and it has been shown<sup>6,7,10,23</sup> to give good performance for many applications in chemistry, and it is useful to know its performance for solids.

This paper is organized as follows. Section II describes the new GGA, and Sec. III gives the computational details of the new calculations performed for this study. Section IV presents results and discusses them, including a survey of the performance of LSDA, eight GGAs (including the new one presented in this article), and two meta-GGAs (including M06-L) for several databases of lattice constants and cohesive energies of solids, bond distances and atomization energies of molecules, barrier heights of chemical reactions, and the exchange energy and total energy of helium atom. Section V concludes this article.

## II. THEORETICAL BACKGROUND

### II.A. GGA exchange and correlation

Let  $n_{\uparrow}$  and  $n_{\downarrow}$  be the up-spin and down-spin electron densities. The exchange energy  $E_x$  for a spin-polarized system ( $n_{\uparrow} \neq n_{\downarrow}$ ) may be evaluated from the exchange functional for a spin unpolarized system ( $n_{\uparrow} = n_{\downarrow}$ ) by using the spin-scaling relation,<sup>24</sup>

$$E_x\{n_{\uparrow}, n_{\downarrow}\} = E_x[2n_{\uparrow}]/2 + E_x[2n_{\downarrow}]/2, \quad (1)$$

where  $E_x[n] \equiv E_x\{n/2, n/2\}$ . Thus, we only need to approximate the exchange energy  $E_x[n]$  of a spin-unpolarized system. In the GGA framework, the exchange energy can be written as

$$E_x^{\text{GGA}}[n] = \int n \varepsilon_x^{\text{LDA}}(n) F_x(s) d^3r, \quad (2)$$

where  $n$  is the electron density ( $n = n_{\uparrow} + n_{\downarrow}$ ),  $s = |\nabla n|/[2(3\pi^2)^{1/3}n^{4/3}]$  is the dimensionless reduced gradient,  $\varepsilon_x^{\text{LDA}}(n) = -3/4(3/\pi)^{1/3}n^{1/3}$  is the exchange energy density per particle for a uniform electron gas (UEG), and  $F_x(s)$  is

the exchange enhancement factor. The second-order density gradient expansion (DGE) of  $F_x(s)$  is<sup>25</sup>

$$F_x^{\text{DGE}} = 1 + \mu^{\text{GE}}s^2 + \dots \quad (s \rightarrow 0), \quad (3)$$

where  $\mu^{\text{GE}} = 10/81 = 0.12346$ . Perdew and co-workers<sup>17,18</sup> showed that obtaining the accurate exchange energy of neutral atoms requires  $\mu \approx 2\mu^{\text{GE}}$  as was used<sup>3</sup> in the PBE exchange functional (and in many functionals popular in chemistry).

The enhancement factor for the PBE (Ref. 3) and PBEsol (Ref. 17) exchange functionals is

$$F_x^{\text{PBE}} = 1 + \kappa \left( 1 - \frac{1}{1 + \frac{\mu s^2}{\kappa}} \right). \quad (4)$$

The parameter  $\mu$  is set to 0.21951 in PBE; this was chosen<sup>3</sup> to make the second-order exchange term cancel the second-order correlation term because the LSDA was believed to be more accurate than the low-order gradient expansion for small  $s$ . Note that this choice of  $\mu$  in PBE exchange disagrees with the second-order term in Eq. (3). In the PBEsol (Ref. 17) exchange functional,  $\mu$  is restored back to  $\mu^{\text{GE}}$  to recover the second-order DGE. The parameter  $\kappa$  is set to 0.804 in PBE and PBEsol, which is a sufficient but not necessary<sup>14</sup> condition to ensure satisfaction of the Lieb–Oxford bound,<sup>20</sup>

$$E_x\{n_{\uparrow}, n_{\downarrow}\} \geq E_{xc}\{n_{\uparrow}, n_{\downarrow}\} \geq \lambda_{\text{LO}} E_x^{\text{LDA}}[n], \quad (5)$$

where  $E_{xc}\{n_{\uparrow}, n_{\downarrow}\}$  is the exchange–correlation energy and  $\lambda_{\text{LO}} = 2.273$ .

For a spin-unpolarized system, the gradient expansion of the correlation energy of a GGA that satisfies the UEG limit is

$$E_c^{\text{GGA}}[n] = \int n \{ \varepsilon_c^{\text{LSDA}}(n) + \beta_c t^2 + \dots \} d^3r, \quad (6)$$

where  $\varepsilon_c^{\text{LSDA}}(n)$  is the correlation energy per particle of the UEG,  $\beta_c$  is a coefficient, and  $t = |\nabla n|/[4(3/\pi)^{1/6}n^{7/6}]$  is the appropriate reduced density gradient for correlation. The value of  $\beta_c$  for the slowly varying high-density limit was obtained by Ma and Brueckner<sup>26</sup>

$$\beta_c^{\text{GE}} = \lim_{n \rightarrow \infty} \beta_c = \beta_{\text{MB}} = 0.066725. \quad (7)$$

In the PBE correlation functional, the gradient expansion is respected, i.e.,  $\beta_c^{\text{PBE}} = \beta_c^{\text{GE}} = 0.066725$ , whereas in PBEsol,  $\beta_c^{\text{PBEsol}}$  is chosen to be 0.046, which is fitted to TPSS (Ref. 9) exchange–correlation energies for a jellium surface. Note that this choice of  $\beta_c^{\text{PBEsol}}$  violates both the gradient expansion of correlation [Eq. (7)] and the PBE choice of cancelling the second-order terms in the DGE for exchange and correlation, which requires<sup>3,17</sup>

$$\beta_c = \frac{3\mu^{\text{GE}}}{\pi^2} = 0.037526. \quad (8)$$

## II.B. The second-order GGA density functional

In the present study, we develop a GGA functional called SOGGA (second-order GGA), for which we enforce a complete restoration of gradient expansion for both exchange and correlation to the second order. In order to satisfy these objectives, we require a more flexible functional form of the exchange GGA. For this purpose, we build on previous work<sup>3,13,14,27</sup> that has led to useful functional forms for the exchange functional, and the reader is referred to the previous work for the justifications of these forms, which are, however—in a final analysis—quite arbitrary since the known constraints on the functional form of the exchange energy leave quite a bit of flexibility. For our purposes, although it is sufficient to take the SOGGA exchange enhancement factor as a half-and-half mixing of the PBE (Ref. 3) and RPBE (Ref. 13) exchange functionals

$$F_x^{\text{SOGGA}} = 1 + \kappa \left( 1 - \frac{1}{2} \frac{1}{1 + \frac{\mu s^2}{\kappa}} - \frac{1}{2} e^{-\mu s^2/\kappa} \right); \quad (9)$$

we choose  $\mu = \mu^{\text{GE}}$  to respect the gradient expansion for exchange [i.e., Eq. (3)]. The parameter  $\kappa$  in SOGGA is determined by enforcing a tighter Lieb–Oxford bound,

$$E_x\{n_\uparrow, n_\downarrow\} \geq \lambda_{\text{ILO}} E_x^{\text{LDA}}, \quad (10)$$

where the parameter  $\lambda_{\text{ILO}} = 1.9555$ , which is the largest value found in the recent work of Odashima and Capelle.<sup>21</sup> Equation (10) will be satisfied if the spin-polarized enhancement factor,  $2^{1/3} F_x(s/2^{1/3})$ , gradually grows with  $s$  to a maximum value less than or equal to  $\lambda_{\text{ILO}}$ ,<sup>3</sup> i.e.,

$$2^{1/3} F_x(s/2^{1/3}) \leq 1.9555 \quad (11)$$

or

$$\kappa \leq 1.9555/2^{1/3} - 1 = 0.552. \quad (12)$$

We choose  $\kappa = 0.552$  according to Eq. (12).

We used the PBE correlation functional in SOGGA because the PBE correlation functional respects the gradient expansion for correlation. Thus, unlike PBE or PBEsol (or any other GGAs known to us), the SOGGA functional completely restores the gradient expansion for both exchange and correlation through second order.

## III. COMPUTATIONAL DETAILS

The SOGGA functional is designed for solids, so we primarily focus on assessing its performance for calculating lattice constants of solids. First, we test SOGGA against a set of equilibrium lattice constants of 18 solids compiled by Staroverov *et al.*,<sup>28</sup> including four main-group metals (Li, Na, K, Al), five semiconductors (C, Si, SiC, Ge, GaAs), five ionic solids (NaCl, NaF, LiCl, LiF and MgO), and four transition metals (Cu, Rh, Pd, and Ag); we label this database of 18 solid-state lattice constants SSLC18. We used the localized Gaussian basis sets tabulated in Table II of Ref. 28 for these 18 solids. We also calculate the cohesive energies of eight solids (C, Si, SiC, Ge, NaCl, NaF, LiCl, and LiF) following the procedure in Ref. 28; this 2004 database of eight solid-state cohesive energies is called SSCE8.

TABLE I. Equilibrium lattice constants ( $\text{\AA}$ ) of the 18 test solids.

Solid	M06-L	SOGGA	Expt. <sup>a</sup>
Li	3.533	3.455	3.451
Na	4.002	4.168	4.210
K	4.980	5.254	5.212
Al	3.971	4.026	4.020
C	3.562	3.561	3.556
Si	5.431	5.442	5.423
SiC	4.348	4.371	4.349
Ge	5.772	5.666	5.646
GaAs	5.744	5.629	5.643
NaCl	5.682	5.595	5.580
NaF	4.606	4.627	4.594
LiCl	5.174	5.045	5.090
LiF	4.023	3.990	3.987
MgO	4.181	4.200	4.197
Cu	3.590	3.566	3.596
Rh	3.896	3.807	3.793
Pd	3.956	3.874	3.877
Ag	4.099	4.030	4.064

<sup>a</sup>From Ref. 28, with an estimate of the zero-point anharmonic expansion removed.

The third test is a ferroelectric material  $\text{PbTiO}_3$ , which has perovskite structure and which is of interest for applications in electronics. The basis sets we used for Pb and Ti are a combination of the LANL effective core potential<sup>29</sup> with the Gaussian-type basis sets from Ref. 30.

We also tested the functionals for the lattice constants of graphite and graphitic BN. We used the 6-31G(*d*) basis set for these two solids.

For the SSLC18 database, we used two atoms per unit cell with 12 000 **k** points for metal solids and 1000 **k** points for others. The solid-state calculations are not spin-polarized.

In addition to the solid-state tests, we performed some new calculations for molecules, transition states, and the helium atom. These calculations all used the MG3S basis set,<sup>31</sup> and all electrons were included (no effective core potentials). The geometries of all molecules and transition states in the AE6 and BH6 databases<sup>32</sup> were optimized at QCISD/MG3 level of theory. The geometries in the MGBL19 database<sup>10</sup> were consistently optimized. For systems with an odd number of electrons and for triplet species, we carried out spin-polarized calculations.

All calculations have been carried out with ultrafine grids using a locally modified GAUSSIAN03 code.<sup>33</sup>

## IV. RESULTS AND DISCUSSION

### IV.A. Solid-state lattice constants

The calculated lattice constants by the M06-L and SOGGA functionals are listed in Table I. The experimental reference data were taken from Ref. 28, with the estimates of the zero-point anharmonic contribution removed so as to yield equilibrium values, that is, the values corresponding to the lowest Born–Oppenheimer electronic energy, including nuclear repulsion. Table I shows that M06-L gives large errors for the lattice constant of the Na and K metals, whereas SOGGA gives very good performance for all 18 solids. The

TABLE II. Errors in equilibrium lattice constants ( $\text{\AA}$ ) of the 18 test solids in Table I.

Methods	Four main-group metals		Five semiconductors		Five ionic solids		Four transition metals		SSLC18	
	MSE	MUE	MSE	MUE	MSE	MUE	MSE	MUE	MSE	MUE
SOGGA	0.002	0.023	0.010	0.016	0.002	0.020	-0.013	0.020	0.001	0.020
PBEsol <sup>a</sup>	-0.003	0.023	0.030	0.030	0.020	0.027	0.000	0.019	0.013	0.025
TPSS <sup>a</sup>	0.053	0.053	0.062	0.062	0.068	0.068	0.025	0.027	0.054	0.054
LSDA <sup>a</sup>	-0.090	0.090	-0.011	0.013	-0.084	0.084	-0.040	0.040	-0.055	0.056
PBE <sup>a</sup>	0.029	0.034	0.079	0.079	0.085	0.085	0.064	0.064	0.066	0.067
M06-L	-0.102	0.142	0.048	0.049	0.044	0.050	0.052	0.056	0.015	0.071

<sup>a</sup>Results for LSDA, PBE, PBEsol, and TPSS are from Ref. 17.

mean errors [both mean signed error (MSE) and mean unsigned error (MUE)] for the SSLC18 database are shown in Table II, where they are divided into four classes, namely, main-group metals, semiconductors, ionic solids, and transition metals. In Table II, we also give errors for the LSDA, PBE, PBEsol, and TPSS functionals that are taken from a recent study of Perdew *et al.*<sup>17</sup> The TPSS density functional makes a particular appropriate comparison because it is a meta-GGA built on PBE.

For the four main-group metals, SOGGA and PBEsol give the best performance, whereas M06-L gives the worst performance due to its severe underestimation of the lattice constants of the Na and K metals (see Table I). For the five semiconductors, LSDA and SOGGA are the best two performers, whereas PBE give the worst performance. SOGGA and PBEsol give the best performance for the five ionic solids and four transition metals, with PBE again worst. Averaged over the 18 solids, SOGGA outperforms PBEsol by 20%. Comparing the performance of the two meta-GGAs, TPSS, and M06-L, we find that TPSS is better for main-group and transition metals, and M06-L is better for semiconductors and ionic solids.

#### IV.B. Energetic databases

The calculated cohesive energies for eight solids are listed in Table III, and the statistical errors are given in Table IV along with the errors for the AE6 (Ref. 32) and BH6 (Ref. 32) databases. AE6 is a representative database of six main-group atomization energies ( $\text{SiH}_4$ ,  $\text{SiO}$ ,  $\text{S}_2$ ,  $\text{C}_3\text{H}_4$ ,  $\text{C}_2\text{H}_2$ , and  $\text{C}_4\text{H}_8$ ), and BH6 is a representative database of six barrier heights for hydrogen transfer reactions (the forward and re-

TABLE III. Cohesive energies (eV/atom) of eight solids.

Solid	M06-L	SOGGA	PBEsol	Expt. <sup>a</sup>
C	7.50	8.50	8.37	7.59
Si	4.69	5.04	4.94	4.68
SiC	6.36	6.94	6.84	6.49
Ge	3.95	4.33	4.28	3.91
NaCl	3.76	3.31	3.33	3.34
NaF	4.23	4.11	4.14	3.98
LiCl	3.91	3.60	3.61	3.59
LiF	4.60	4.62	4.64	4.47

<sup>a</sup>These are equilibrium values derived from the 0 K cohesive energy of Ref. 28, with an estimate of the zero-point contributions from the Debye temperature  $\Theta_D$  ( $E_{ZPE} = 9/8k_B\Theta_D$ ).

verse barriers of  $\text{OH} + \text{CH}_4 \rightarrow \text{CH}_3 + \text{H}_2\text{O}$ ,  $\text{H} + \text{OH} \rightarrow \text{O} + \text{H}_2$ , and  $\text{H} + \text{H}_2\text{S} \rightarrow \text{HS} + \text{H}_2$ ). Inclusion of these databases allows us to compare small-molecule energetics to solid-state cohesive energies. Since SOGGA and PBEsol restore the gradient expansion for exchange, they are not accurate for the energies of atoms, which is consistent with the conclusion of Perdew and co-workers<sup>17,18</sup> that one needs  $\mu \approx 2\mu^{\text{GE}}$  for accurate energies of atoms (both SOGGA and PBEsol have  $\mu = \mu^{\text{GE}}$ ). Table IV shows that SOGGA and PBEsol are less accurate than PBE for cohesive energies, atomization energies, and barrier heights. The best performer in Table IV is M06-L, which was designed for thermochemistry, kinetics, and noncovalent interactions.

#### IV.C. PbTiO<sub>3</sub>

PbTiO<sub>3</sub> is a prototype ferroelectric perovskite crystal with a high-temperature cubic phase and a low-temperature phase of tetragonal symmetry ( $P4mm$ ). Recently Wu *et al.* employed the linearized augmented plane wave method with local orbital extensions<sup>34</sup> (LAPW+LO) to compare the weighted density approximation with LDA and the PBE GGA. They found that PbTiO<sub>3</sub> is a difficult case for both LDA and PBE. We calculated the lattice constants for the cubic phase and tetragonal phase, and the results are shown in Table V. The experimental reference data in Table V are for 0 K, which we extrapolated from the low-temperature data of Mabud and Glazer.<sup>35</sup> Although these are not equilibrium lattice constants, and they are not as accurate as the reference data in Table I, they are accurate enough for the present comparisons.

For the cubic phase, SOGGA and PBEsol gives the best agreement with experiment, whereas PBE, TPSS, and M06-L

TABLE IV. Errors in cohesive energies (eV/atom) for the eight solids in Table III, in the AE6 database (eV/bond), and in the BH6 database (eV).

Method	SSCE8		AE6		BH6		AMUE <sup>a</sup>
	MSE	MUE	MSE	MUE	MSE	MUE	
M06-L	0.12	0.17	0.02	0.03	-0.18	0.19	0.13
TPSS	0.17	0.22	0.03	0.05	-0.36	0.36	0.21
PBE	-0.04	0.11	0.10	0.13	-0.40	0.40	0.22
PBEsol	0.26	0.27	0.31	0.31	-0.55	0.55	0.38
SOGGA	0.30	0.31	0.30	0.32	-0.57	0.57	0.40
LSDA	0.70	0.70	0.69	0.69	-0.77	0.77	0.72

<sup>a</sup>AMUE is the average of three MUE columns.

TABLE V. Lattice constants ( $\text{\AA}$ ) for the cubic and tetragonal phases of  $\text{PbTiO}_3$ .

Method	Cubic		Tetragonal		MSE	MUE
	$a$	$a=b$	$c$			
Expt. <sup>a</sup>	3.911	3.878	4.174			
SOGGA	3.913	3.869	4.139	-0.014	0.015	
M06-L	3.950	3.906	4.170	0.021	0.024	
PBEsol	3.921	3.861	4.236	0.018	0.030	
TPSS	3.957	3.884	4.459	0.112	0.112	
PBE	3.958	3.845	4.612	0.151	0.173	

<sup>a</sup>The experimental data were extrapolated from the low-temperature data of Mabud and Glazer (Ref. 35).

overestimate the lattice constant by a large margin. For the tetragonal phase, M06-L and PBEsol are the best two performers. Averaging over three lattice constants of  $\text{PbTiO}_3$ , we find that SOGGA gives the best performance, followed by M06-L.

#### IV.D. Graphite and graphitic BN

Graphite and graphitic BN deviate more strongly from the uniform electron gas than the solids studied in Secs. IV.A–IV.C, and most of the standard GGAs and meta-GGAs are questionable<sup>5,6,36</sup> for the prediction of the interlayer  $\pi \cdots \pi$  interactions in these solids. The reference experimental lattice constants were taken from the literature.<sup>37,38</sup> As shown in Table VI, all tested density functionals give reasonable performance for the intralayer lattice constants (maximum error is only 0.016  $\text{\AA}$ ), but all the tested functional except M06-L give large errors for the interlayer lattice constants. Averaged over four lattice constants, M06-L is the best performer, and both SOGGA and PBEsol improve upon the PBE and TPSS functionals.

#### IV.E. Benchmarking popular GGAs for solids

In order to place the present results in a broader perspective we applied five additional GGAs to three of the test cases of Tables I and II; in particular, PW91,<sup>39</sup> mPWPW,<sup>40</sup> BPW91 [B88 (Ref. 41) for exchange and PW91 (Ref. 39) for correlation], BLYP [B88 (Ref. 41) for exchange and LYP (Ref. 42) for correlation], and RPBE<sup>13</sup> were applied to K, NaCl, and Si. This subset of SSLC18 is called SSLC3. (Note

TABLE VI. Equilibrium lattice constants ( $\text{\AA}$ ) for graphite and graphitic BN.

Methods	Graphite ( $A_9$ )		BN ( $B_8$ )		MSE	MUE
	$a_0$	$c_0$	$a_0$	$c_0$		
Expt. <sup>a</sup>	2.459	6.672	2.504	6.652		
M06-L	2.462	6.691	2.502	6.540	-0.023	0.034
SOGGA	2.467	7.125	2.510	6.958	0.193	0.193
PBEsol	2.468	7.157	2.511	6.981	0.207	0.207
PBE	2.475	7.290	2.518	7.266	0.315	0.315
TPSS	2.474	7.266	2.518	8.109	0.520	0.520

<sup>a</sup>Experimental data for graphite are taken from Ref. 37, and those for graphitic BN from Ref. 38. The intralayer lattice constant is  $a_0$  and the interlayer lattice constant is  $c_0$ .

TABLE VII. Comparison of GGAs and LSDA for the lattice constants ( $\text{\AA}$ ) of K, NaCl, and Si.

Method	K	NaCl	Si	MUE
Expt.	5.212	5.580	5.423	
SOGGA	5.254	5.595	5.442	0.025
PBEsol	5.240	5.597	5.454	0.025
LSDA	5.093	5.471	5.426	0.077
PW91	5.308	5.682	5.488	0.088
PBE	5.308	5.698	5.490	0.094
mPWPW <sup>a</sup>	5.340	5.710	5.492	0.109
BPW91	5.367	5.733	5.494	0.126
BLYP	5.368	5.756	5.553	0.154
RPBE	5.444	5.819	5.519	0.189

<sup>a</sup>Also sometimes called mPWPW91.

that all the GGAs in Table VII except BLYP and PBEsol use either the PW91 or the PBE functional for correlation; since those two correlation functionals have only a minor difference, the comparisons of SOGGA, PW91, PBE, mPWPW, and RPBE are essentially a test of varying only the exchange functional.) Table VII confirms that, in keeping with the goals that motivated their designs, SOGGA and PBEsol perform better for solid-state lattice constants than other popular GGAs.

#### IV.F. Synthesis

We have prepared one more table (Table VIII); by considering this table along with Tables IV–VI, we hope to achieve a synthesis of our conclusions. Table VIII includes a column for  $\mu$ , defined as

$$\mu \equiv \lim_{s \rightarrow 0} \left( \frac{1}{2} \frac{d^2 F_x}{ds^2} \right). \quad (13)$$

However, the value of  $\mu$  requires further discussion for PW91 and mPWPW91. For the PW91 functional

$$\lim_{s \rightarrow 0} \left( \frac{1}{2} \frac{d^2 F_x}{ds^2} \right) \rightarrow 0.2743 - 0.1508e^{-100s^2}. \quad (14)$$

Thus, PW91 has the correct second-order gradient expansion but only in the very small range of  $s$ . The mPWPW91 exchange is a modified version of PW91, and it has the same behavior as PW91. To indicate that formally  $\mu$  is 0.1235 but for practical purposes it is 0.2743,  $\mu$  for these functionals is listed as “0.12(0.27)” in Table VIII.

The next three columns in Table VIII, namely, SSLC3, AE6, and BH6, have already been described. These three columns, along with Table V and the intralayer results in Table VI show that low- $\mu$  GGAs (namely, PBEsol and SOGGA) are more accurate for solid-state lattice constants and less accurate for small-molecule energetics with the opposite trend for large- $\mu$  GGAs (PBE, BPW91, BLYP, and RPBE). This conclusion is fully consistent with the work of Perdew and coworkers,<sup>17,18,43,44</sup> which motivated the present study. Madsen<sup>45</sup> similarly emphasized the competing objectives of improving atomic exchange energies versus improving equilibrium volumes of dense solids. An example of this perspective is the work of Csonka *et al.*,<sup>22</sup> which contrasts

TABLE VIII. Mean unsigned errors in energies (in eV) and distances (Å).

Method	$\mu$	SSLC3 <sup>a</sup> (Å)	AE6 (eV/bond)	BH6 (eV)	SF <sub>6</sub>		MGBL19 (Å) <sup>d</sup>		He	
					$D_e$ (eV) <sup>b</sup>	$R_e$ (Å) <sup>c</sup>	MGHBL9	MGNHBL10	$E_x$ (eV) <sup>e</sup>	$E_{\text{tot}}$ (eV) <sup>f</sup>
GGAs and LSDA										
SOGGA	0.1235	0.025	0.32	0.57	3.85	0.020	0.015	0.006	2.02	1.58
PBEsol	0.1235	0.025	0.31	0.55	3.67	0.022	0.014	0.006	2.01	1.30
LSDA	0	0.077	0.69	0.77	7.29	0.008 <sup>g</sup>	0.015	0.005	4.62	3.72
PW91	0.12(0.27) <sup>h</sup>	0.088	0.14	0.42	1.36	0.033	0.010	0.007	0.46	0.14
PBE	0.2195	0.094	0.13	0.40	1.18	0.035	0.011	0.008	0.58	0.34
mPWPW91	0.12(0.27) <sup>h</sup>	0.109	0.09	0.37	0.72	0.035	0.009	0.008	0.28	0.00
BPW91	0.2743	0.126	0.06	0.32	0.18	0.036	0.010	0.008	0.17	0.08
BLYP	0.2743	0.154	0.06	0.34	0.43 <sup>i</sup>	0.048	0.010	0.015	0.22	0.05
RPBE	0.2195	0.189	0.09	0.28	0.93 <sup>i</sup>	0.045	0.011	0.013	0.02	0.15
meta-GGAs										
TPSS	0.2195	0.107	0.05	0.36	0.07	0.029	0.007	0.007	0.05	0.12
M06-L	0.2195	0.114	0.03	0.19	0.50	0.007	0.002	0.004	0.37	0.21

<sup>a</sup>Mean unsigned error for three lattice constants in Table VII.

<sup>b</sup>Unsigned error for the total bond dissociation energies, the experimental reference value is 20.71 eV.

<sup>c</sup>Unsigned error for the S–F bond length, and the best estimate is 1.561 Å from Kuchitsu (Ref. 47).

<sup>d</sup>A database of 19 bond lengths of main group compounds. See Ref. 10 for details.

<sup>e</sup>Unsigned error for the exchange energy of the He atom, and the best estimate is –27.914 eV from Kurth (Ref. 44).

<sup>f</sup>Unsigned error for the total energy of the He atom, and the best estimate is –79.015 eV from Chakravorty (Ref. 48).

<sup>g</sup>This value negative; all other values in this column positive.

<sup>h</sup>See Eq. (4) in text.

<sup>i</sup>These values negative; all other values in this column positive.

the density functional requirements of atoms and small molecules to those of solids. Next, we try to improve this perspective.

The next two columns of Table VIII involve the atomization energy (called  $D_e$ ) and equilibrium S–F bond length (called  $R_e$ ) for the main-group gas-phase molecule SF<sub>6</sub>. While AE6 involves atoms with coordination numbers of 1–4, the solids of Table I have coordination number of 8 (for body-centered-cubic potassium), 6 (for NaCl), and 4 (for Si). SF<sub>6</sub> is a small molecules with an unusually large coordination number of 6 for the central S. Table VIII nevertheless shows that the trend in errors in the atomization energy of SF<sub>6</sub> (high- $\mu$  better) parallels the trends in AE6, and the trend in errors in bond length (small- $\mu$  better) parallel that for SSLC3. Furthermore the trend in both the SF<sub>6</sub> atomization energy and AE6 parallel the trend in the energetics of SSCE8 (Table IV), and the trend in SF<sub>6</sub> bond length parallels the trend for PbTiO<sub>3</sub> lattice constants (Table V) and graphite and graphitic BN intralayer lattice constants (Table V). To this point we see that low- $\mu$  GGAs are consistently more accurate for interatomic spacings (except the noncovalent weak ones in Table VI) in either lattices or small-molecule bonds, and high- $\mu$  GGAs are more accurate for both solid-state cohesive energies and small-molecule energetics.

To further examine these correlations we turn to a previously developed<sup>10</sup> database of 19 main-group small-molecule bond lengths, MGBL19. This database can be divided into MGHBL9 with nine hydrogenic bond lengths (HBLs) and MGNHBL10 with ten nonhydrogenic bond lengths (NHBLs). The mean unsigned errors are shown in Table VIII. We find similar trends in nonhydrogenic bond lengths to those in lattice constants (small- $\mu$  better), but hydrogenic bond lengths show the opposite trend in accuracy with varying  $\mu$ .

The last two columns of Table VIII give the errors in the exchange energy and total energy of the He atom. We see that large  $\mu$  is better, as for all other energetic quantities in this article. We can summarize the synthesis for the performance of GGA exchange functionals: A wide variety of lattice constants and bond distances show improved accuracy when  $\mu$  is close to the gradient expansion value of  $\sim 0.12$ , with the only exception being hydrogenic bond lengths. An even wider variety of energetic quantities (cohesive energies of diverse solids, atomization energies of small molecules, barrier heights of chemical reactions, and the exchange energy and total energy of He atom) are improved when  $\mu$  is about twice as large.

The two meta-GGAs in Table VIII are both high- $\mu$  functionals. For the most part, they show similar trends to the high- $\mu$  GGAs, the most notable differences being encouragingly improved accuracy for AE6 and both kinds of main-group bond lengths.

Zupan *et al.*<sup>46</sup> showed that the average value of  $s$  for a number of atoms, small molecules, and solids is in the range of 0.6–1.1 and that most atomic and molecular properties depend on  $s$  values in the range of  $0 \leq s \leq 3$ . (They did not consider noncovalent forces, which can be sensitive to larger  $s$ .) Similarly Hammer *et al.*<sup>13</sup> found that the critical range of  $s$  for chemisorption energies of CO on Pd surface is  $0.5 \leq s \leq 2.5$ . Figure 1 shows the exchange enhancement factor  $F_x$  for seven of the GGAs considered in this article. The separation of the curves into two low- $\mu$  functionals and five high- $\mu$  functionals is readily apparent. Examination of the terms in the gradient expansion shows that the second-order expansion usually determines the magnitude of the enhancement factors out to  $s \approx 0.5$ , after which the higher terms become noticeable.

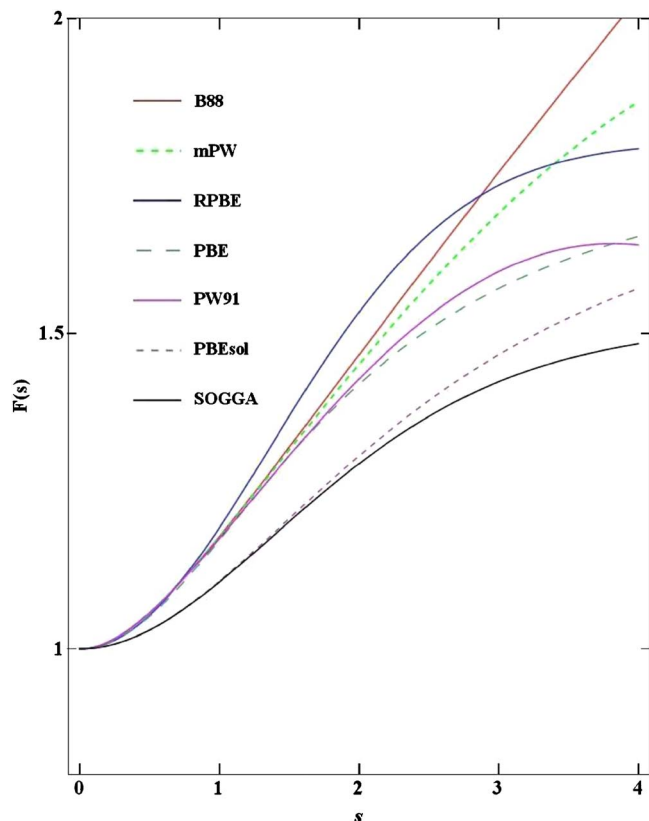


FIG. 1. (Color online) Exchange enhancement factors  $F_x$  for SOGGA, PBEsol, and other popular GGAs. The curve labels are listed in the same order as the value of  $F_x$  at the right-hand edge of the plot.

In comparing SOGGA to the PBEsol functional, we should keep in mind that the developers of PBEsol intentionally violated the correct second-order gradient expansion to improve jellium surface energies. In contrast, we did not consider jellium surface energies but rather based the new functional on universal properties. The practical results obtained in this way for equilibrium interatomic distances in both solids and molecules are encouraging.

## V. CONCLUDING REMARKS

We developed a new GGA by a combination of a complete restoration of the gradient expansion through second order for both exchange and correlation and enforcing a tighter Lieb–Oxford bound. The construction of the new GGA follows a nonempirical “constraint satisfaction” approach<sup>19</sup> without fitting to data sets. The resulting SOGGA functional satisfies one more exact constraint than the PBEsol functional, and it becomes exact for slowly-varying densities. The new functional involves three modifications to the PBE generalized gradient approximation for exchange, namely (a) replacement of the PBE enhancement factor by a 50:50 mixture of the PBE and RPBE enhancement factors, (b) changing the value of the parameter  $\mu$  from 0.21591 to 10/81 in order to restore the correct second-order gradient expansion, the benefit of which was pointed out recently by Perdew *et al.*,<sup>17</sup> and (c) tightening the Lieb–Oxford bound by lowering the value of the parameter  $\kappa$  from 0.804 to 0.552. These three modifications are made in concert, and it would

be an oversimplification to say that any one of them is chiefly responsible for the better performance we observe.

SOGGA performs slightly better (on average) than PBEsol for the lattice constants in 18 previously studied solids including four simple metals, five semiconductors, five ionic solids, and four transition metals. It is also shown that SOGGA performs slightly better than PBEsol for the lattice constants of the cubic and tetragonal phases of the  $\text{PbTiO}_3$  ferroelectric perovskite crystal and for the lattice constants of graphite and graphitic BN.

We also tested the performance of the meta-GGA M06-L, which has previously been shown to provide very good performance for small-molecule chemistry. Although M06-L underestimates the lattice constants of the Na and K metals by a large margin, it performs better than PBE for semiconductors, ionic solids, and transition metals. M06-L gives the best performance of five tested functionals for graphite and graphitic BN.

Finally, we noted a trend in which low- $\mu$  GGAs tend to give more accurate nonhydrogenic interatomic distances, and high- $\mu$  GGAs tend to give more accurate energetics, with these trends being observed both in the solid state and in small molecules in the gas phase.

## ACKNOWLEDGMENTS

The authors are grateful to Viktor N. Staroverov for the help with the GAUSSIAN03 input files for the SSLC18 database. This work was supported, in part, by the National Science Foundation under Grant No. CHE07-04974 (complex systems), by the Office of Naval Research under Award No. N00014-05-0538 (software tools), and by a Molecular Science Computing Facility Computational Grand Challenge grant at Environmental Molecular Science Laboratory of Pacific Northwestern National Laboratory.

- P. Hohenberg and W. Kohn, *Phys. Rev.* **136**, 864 (1964); W. Kohn and L. J. Sham, *ibid.* **140**, 1133 (1965).
- W. Kohn, *Rev. Mod. Phys.* **71**, 1253 (1999).
- J. P. Perdew, K. Burke, and M. Ernzerhof, *Phys. Rev. Lett.* **77**, 3865 (1996).
- A. D. Becke, *J. Chem. Phys.* **98**, 1372 (1993); **98**, 5648 (1993); C. Adamo and V. Barone, *ibid.* **110**, 6158 (1999).
- Y. Zhao, N. E. Schultz, and D. G. Truhlar, *J. Chem. Theory Comput.* **2**, 364 (2006).
- Y. Zhao and D. G. Truhlar, *Theor. Chem. Acc.* **120**, 215 (2008). See also erratum in *Theor. Chem. Acc.* **119**, 525(2008).
- Y. Zhao and D. G. Truhlar, *Acc. Chem. Res.* **41**, 157 (2008).
- A. D. Becke, *J. Chem. Phys.* **104**, 1040 (1996).
- J. Tao, J. P. Perdew, V. N. Staroverov, and G. E. Scuseria, *Phys. Rev. Lett.* **91**, 146401 (2003).
- Y. Zhao and D. G. Truhlar, *J. Chem. Phys.* **125**, 194101 (2006).
- M. Gruning, O. Gritsenko, and E. J. Baerends, *J. Phys. Chem. A* **108**, 4459 (2004).
- S. K. Ghosh and R. G. Parr, *Phys. Rev. A* **34**, 785 (1986); A. D. Becke, *J. Chem. Phys.* **88**, 1053 (1988); R. M. Koehl, G. K. Odom, and G. E. Scuseria, *Mol. Phys.* **87**, 835 (1996); J. P. Perdew, S. Kurth, A. Zupan, and P. Blaha, *Phys. Rev. Lett.* **82**, 2544 (1999).
- B. Hammer, L. B. Hansen, and J. K. Norskov, *Phys. Rev. B* **59**, 7413 (1999).
- Y. Zhang and W. Yang, *Phys. Rev. Lett.* **80**, 890 (1998).
- G. K. H. Madsen, *Phys. Rev. B* **75**, 195108 (2007).
- Z. Wu and R. E. Cohen, *Phys. Rev. B* **73**, 235116 (2006); see also Y. Zhao and D. G. Truhlar (to be published) for discussion of their derivation.
- J. P. Perdew, A. Ruzsinszky, G. I. Csonka, O. A. Vydrov, G. E. Scuseria,

- L. A. Constantin, X. Zhou, and K. Burke, *Phys. Rev. Lett.* **100**, 136406 (2008).
- <sup>18</sup>J. P. Perdew, L. A. Constantin, E. Sagvolden, and K. Burke, *Phys. Rev. Lett.* **97**, 223002 (2006).
- <sup>19</sup>J. P. Perdew, A. Ruzsinszky, J. Tao, V. N. Staroverov, G. E. Scuseria, and G. I. Csonka, *J. Chem. Phys.* **123**, 062201 (2005).
- <sup>20</sup>E. H. Lieb and S. Oxford, *Int. J. Quantum Chem.* **19**, 427 (1981).
- <sup>21</sup>M. M. Odashima and K. Cappelle, *J. Chem. Phys.* **127**, 054106 (2007).
- <sup>22</sup>G. I. Csonka, O. A. Vydrov, G. E. Scuseria, A. Ruzsinszky, and J. P. Perdew, *J. Chem. Phys.* **126**, 244107 (2007).
- <sup>23</sup>Y. Zhao and D. G. Truhlar, *Org. Lett.* **9**, 1967 (2007).
- <sup>24</sup>G. L. Oliver and J. P. Perdew, *Phys. Rev. A* **20**, 397 (1979).
- <sup>25</sup>P. R. Antoniewicz and L. Kleinman, *Phys. Rev. B* **31**, 6779 (1985).
- <sup>26</sup>S.-K. Ma and K. A. Brueckner, *Phys. Rev.* **165**, 18 (1968).
- <sup>27</sup>A. D. Becke, *J. Chem. Phys.* **84**, 4524 (1986).
- <sup>28</sup>V. N. Staroverov, G. E. Scuseria, J. Tao, and J. P. Perdew, *Phys. Rev. B* **69**, 075102 (2004).
- <sup>29</sup>P. J. Hay and W. R. Wadt, *J. Chem. Phys.* **82**, 299 (1985).
- <sup>30</sup>S. Piskunov, E. Heifets, R. I. Eglitis, and G. Borstel, *Comput. Mater. Sci.* **29**, 165 (2004).
- <sup>31</sup>B. J. Lynch, Y. Zhao, and D. G. Truhlar, *J. Phys. Chem. A* **107**, 1384 (2003).
- <sup>32</sup>B. J. Lynch and D. G. Truhlar, *J. Phys. Chem. A* **107**, 8996 (2003); **108**, 1460(E) (2004).
- <sup>33</sup>M. J. Frisch, G. W. Trucks, H. B. Schlegel *et al.*, GAUSSIAN03, Revision D.01, Gaussian, Inc., Pittsburgh, PA, 2004.
- <sup>34</sup>D. J. Singh, *Planewaves, Pseudopotentials and LAPW Method* (Kluwer, Boston, 1994).
- <sup>35</sup>S. A. Mabud and A. M. Glazer, *J. Appl. Crystallogr.* **12**, 49 (1979).
- <sup>36</sup>Y. Zhao and D. G. Truhlar, *J. Phys. Chem. A* **109**, 5656 (2005); *J. Chem. Theory Comput.* **2**, 1009 (2006).
- <sup>37</sup>R. S. Peace, *Acta Crystallogr.* **5**, 356 (1952).
- <sup>38</sup>Y. Baskin and L. Meyer, *Phys. Rev.* **100**, 544 (1955).
- <sup>39</sup>J. P. Perdew, in *Electronic Structure of Solids '91*, edited by P. Ziesche and H. Eschig (Akademie, Berlin, 1991), p. 11.
- <sup>40</sup>C. Adamo and V. Barone, *J. Chem. Phys.* **108**, 664 (1998).
- <sup>41</sup>A. D. Becke, *Phys. Rev. A* **38**, 3098 (1988).
- <sup>42</sup>C. Lee, W. Yang, and R. G. Parr, *Phys. Rev. B* **37**, 785 (1988).
- <sup>43</sup>J. P. Perdew, K. Burke, and M. Ernzerhof, *Phys. Rev. Lett.* **80**, 891 (1998).
- <sup>44</sup>S. Kurth, J. P. Perdew, and P. Blaha, *Int. J. Quantum Chem.* **75**, 889 (1999).
- <sup>45</sup>G. K. H. Madsen, *Phys. Rev. B* **75**, 195108 (2007).
- <sup>46</sup>A. Zupan, K. Burke, M. Ernzerhof, and J. P. Perdew, *J. Chem. Phys.* **106**, 10184 (1997).
- <sup>47</sup>K. Kuchitsu, *Structure of Free Polyatomic Molecules-Basic Data* (Springer, Berlin, 1998).
- <sup>48</sup>S. J. Chakravorty, S. R. Gwaltney, E. R. Davidson, F. A. Parpia, and C. F. F. Fischer, *Phys. Rev. A* **47**, 3649 (1993).